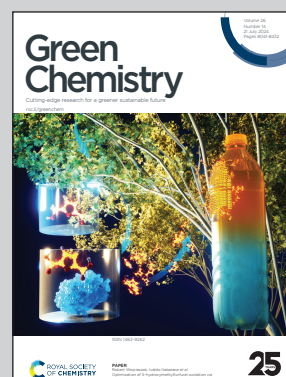


**Showcasing research presented by Professor Jaewook Myung and Hanseul Yang from KAIST, and Professor Jongchul Seo from Yonsei University, Republic of Korea.**

**Boric acid-crosslinked poly(vinyl alcohol): biodegradable, biocompatible, robust, and high-barrier paper coating**

Traditional coating materials for paper packaging exacerbate plastic pollution, prompting the need for sustainable alternatives. A biodegradable, biocompatible, robust, and high-barrier paper coating material was developed to tackle the challenge of balancing packaging performance and sustainability. The boric acid-crosslinked polyvinyl alcohol coating remarkably improves barrier properties and mechanical robustness without compromising biodegradability and biocompatibility of paper, marking a green advance in sustainable packaging.

**As featured in:**



See Jaewook Myung *et al.*,  
*Green Chem.*, 2024, **26**, 8230.



Cite this: *Green Chem.*, 2024, **26**, 8230

## Boric acid-crosslinked poly(vinyl alcohol): biodegradable, biocompatible, robust, and high-barrier paper coating†

Shinhyeong Choe,<sup>a</sup> Seulki You,<sup>b</sup> Kitae Park,<sup>c</sup> Youngju Kim,<sup>a,b</sup> Jehee Park,<sup>a</sup> Yongjun Cho,<sup>a</sup> Jongchul Seo,<sup>c</sup> Hanseul Yang<sup>b</sup> and Jaewook Myung<sup>\*a</sup>

The accumulation of plastic packaging wastes in the natural environment highlights the significance of sustainable alternatives. Paper is widely used as a biodegradable packaging material, but poor mechanical strength, barrier properties, and water resistance limit its utility. Typical paper coating materials applied to overcome such drawbacks, such as polyethylene (PE) and ethylene vinyl alcohol (EVOH), are not desirable for sustainability due to environmental persistence. Here, we report a biodegradable, biocompatible, robust, and high-barrier paper coating strategy using boric acid-crosslinked poly(vinyl alcohol) (PVA). Various crosslinked-PVA solutions were prepared using boric acid (BA) and hydrochloric acid (HCl) as a crosslinker and an acid catalyst, respectively. The solutions were coated onto the Kraft paper (KP) through facile bar coating with epichlorohydrin (ECH) as a binder (henceforth referred to as coated papers). The coated papers (KP-P, KP-PB, KP-PBH) show remarkably improved oxygen ( $\sim 0.89 \text{ cc m}^{-2} \text{ d}^{-1}$ ) and water vapor ( $\sim 5.17 \text{ g m}^{-2} \text{ d}^{-1}$ ) barrier properties as well as tensile strength ( $\sim 53.0 \text{ MPa}$ ) that is retained in moist conditions. The coated papers were significantly mineralized into  $\text{CO}_2$  (59.2–81.6% over 111 d) in the simulated marine environment biodegradation test. Depolymerization of polymer chains and surface degradation of coated papers are evidenced *via* FT-IR and SEM, respectively. The microcosm test revealed that the intensive disintegration of the coated papers is synergistically driven by both biotic and abiotic factors (*i.e.*, mechanical stress). Moreover, the *in vitro* biocompatibility tests employing human embryonic kidney and mouse embryonic fibroblast cells, and *in vivo* biocompatibility test with mice suggest that the coated papers are highly biocompatible. This work provides a promising strategy for paper packaging that enhances packaging performance without compromising environmental sustainability.

Received 2nd February 2024,  
 Accepted 8th April 2024

DOI: 10.1039/d4gc00618f

rsc.li/greenchem

## Introduction

End-of-use plastic materials are accumulated in freshwater and marine ecosystems.<sup>1–3</sup> It is estimated that 1.15–2.41 million tons of plastic waste enter the ocean from rivers annually.<sup>4</sup> Plastic debris, including single-use packaging material, endangers marine fauna through ingestion and entanglement.<sup>5–8</sup> Moreover, once the plastic waste is leaked into the natural environment, it readily fragments into microplastics (<5 mm), which can threaten the marine ecosystem from tiny microor-

ganisms such as plankton<sup>5</sup> to relatively bigger animals like fish,<sup>6,7</sup> shellfish,<sup>9</sup> and birds.<sup>8,10</sup>

Since packaging accounts for 31% of global plastic consumption, biodegradable packaging material has been of particular interest.<sup>11–13</sup> Paper is widely used as a biodegradable packaging material, yet its practical application is limited due to poor water resistance, oxygen and vapor barrier properties, and mechanical strength.<sup>14</sup> Surface coating technique is a well-established commercial practice to impart the desired property to paper.<sup>15</sup> Currently, petroleum-based synthetic polymers, including polyethylene (PE), polypropylene (PP), and ethylene vinyl alcohol (EVOH) are extensively employed to increase the barrier properties of paper-based packaging.<sup>16</sup> However, these non-degradable barrier coatings can bring about environmental pollution and potential health issues.<sup>13,17</sup>

Bio-based barrier coatings are garnering rising attention due to various merits including biodegradability, biocompatibility, low toxicity, and structural flexibility.<sup>18</sup> Particularly, bio-

<sup>a</sup>Department of Civil and Environmental Engineering, KAIST, Daejeon, 34141, Republic of Korea. E-mail: jjaimyung@kaist.ac.kr

<sup>b</sup>Department of Biological Sciences, KAIST, Daejeon, 34141, Republic of Korea

<sup>c</sup>Department of Packaging & Logistics, Yonsei University, 1 Yonsei-dae-gil, Wonju-si, Gangwon-do 26493, Republic of Korea

† Electronic supplementary information (ESI) available. See DOI: <https://doi.org/10.1039/d4gc00618f>



degradable plastics, which can be incorporated into the natural carbon cycle, hold the potential to prevent plastic accumulation in nature.<sup>19–22</sup> Therefore, the development of biodegradable coating material that improves barrier and mechanical properties is essential.

Several research have shown promising developments in the field of sustainable packaging materials. Recently, a newspaper-based composite enhanced by borate ester (B–O–C) bonds that features high mechanical, self-healing properties, and full degradability was reported.<sup>23</sup> Chitosan-based cardanol glycidyl ether was studied as a paper coating material, featuring water and oil resistance, recyclability, UV-shielding, and biodegradability.<sup>24</sup> Rosin-grafted cellulose composite paper with water resistance, robustness, degradability, and recyclability was researched.<sup>25</sup> Another group developed a multilayer packaging assembly consisting of paper, thermoplastic starch (TPS), and a thin layer of polylactic acid (PLA), poly(butylene adipate-*co*-terephthalate) (PBAT), or poly(3-hydroxybutyrate-*co*-3-hydroxyvalerate) (PHBV).<sup>26</sup> In our earlier studies, we reported that the introduction of boric acid (BA) to poly(vinyl alcohol) (PVA) forms covalently-bonded borate ester crosslinks between the PVA chains and hydrochloric acid (HCl) catalyst significantly increased the crosslinking density.<sup>27,28</sup> This in turn resulted in significant enhancement in oxygen and vapor barrier properties, water resistance, and tensile strength of PVA.

Nonetheless, despite these advancements, there is a notable gap in studies that quantitatively assess the biodegradability of high-performance packaging materials.<sup>27–31</sup> The extent of organic material biodegradation should be assessed based on the mineralization of carbon into CO<sub>2</sub>.<sup>32–34</sup> However, many previous studies have relied on weight attrition or visual inspection to evaluate biodegradation. These methods do not guarantee a material's complete end-of-life scenario.<sup>35–37</sup>

Biodegradable plastics often fail to meet design criteria such as barrier properties and mechanical robustness for packaging applications, rendering them unattractive compared to their established non-degradable counterparts.<sup>38,39</sup> Blending or fabricating composites of non-biodegradable materials with biodegradable plastics is a common strategy intended to alleviate the environmental impact (*e.g.*, PE coating on the paper cup). Importantly, such practice can inadvertently generate millions of micro- and nanoplastics due to partial degradation, exacerbating environmental pollution.<sup>36,40</sup> Taking into account the environmental persistence of plastic in material design could result in significant societal benefits, potentially amounting to hundreds of millions of dollars for a single consumer product.<sup>41</sup> Given these environmental concerns, it is crucial to strike a balance between performance and biodegradability to fully realize the advantages of utilizing biodegradable materials.<sup>38</sup>

Here, we present biodegradable, biocompatible, robust, and high-barrier BA-crosslinked PVA for paper coating. The cross-linked PVA solutions with different compositions were coated onto the Kraft paper (KP) *via* facile bar coating (henceforth referred to as coated papers). The introduction of BA-cross-

linked PVA coating complements the poor oxygen and water vapor barrier and mechanical properties of papers. In addition, we systematically evaluated the sustainability of the coated papers (KP-P, KP-PB, KP-PBH). We performed (1) marine biodegradation test by analyzing mineralization levels and (2) *in vitro* and *in vivo* biocompatibility tests employing cells and mice. For the first time, we demonstrate that the BA-crosslinked PVA coating improves the barrier and mechanical properties of paper and the coated papers are biodegradable in the marine environment and highly biocompatible. This work presents a promising strategy for successful paper packaging that improves material performance while retaining environmental sustainability.

## Results and discussion

### Fabrication, morphology, and chemical structure

The PVA solutions with different compositions were prepared with BA crosslinker and HCl catalyst, and they were coated onto the KP with epichlorohydrin (ECH) as a binder using facile bar coating apparatus (Fig. 1a). KP was used as paper substrate due to its high stability, mechanical strength, versatility, and universality.<sup>42</sup> BA induces the crosslinks among PVA chains and this is further intensified with HCl catalyst.<sup>27</sup> ECH was employed as a coating agent to induce crosslinking bonds between cellulose fibers in KP and PVA.<sup>43</sup> The coated papers (KP-P, KP-PB, and KP-PBH, Table 1) exhibit a smooth and slightly waxy texture compared to pristine KP (Fig. 1a). SEM images of coated papers show that the PVA coating solutions form homogenous layer onto the KP (Fig. 1b). The top-view surface morphology exhibits the plain surface morphology of PVA. In the cross-sectional images, PVA coating solutions formed a PVA-cellulose layer with irregular interfaces, suggesting the formation of covalent crosslinking bonds between KP and PVA induced by ECH binder (Fig. 1b).

Fourier-transform infrared spectroscopy (FT-IR) curves of coated papers also indicate that BA-crosslinked PVA were successfully coated onto the KP (Fig. 2). The peaks in stretching vibration of –OH at 3300–3600 cm<sup>–1</sup>, wagging vibration and –CH at 1416 cm<sup>–1</sup>, and symmetric stretching vibration of –CH<sub>2</sub> at 2908 cm<sup>–1</sup> are the characteristic bonds of PVA. When BA is added to PVA, crosslinking bonds are formed between hydroxyl groups of PVA and borate ions (Fig. 2b).<sup>23,44</sup> The new bands of methaboric acid vibration at 770 cm<sup>–1</sup> and BO<sub>3</sub> symmetric deformation vibration at 659–663 cm<sup>–1</sup> evidence the borate ester crosslinks in KP-PB and KP-PBH.<sup>44</sup> The –OH groups within the repetitive units of PVA served as reactive sites, enabling interactions with hydrolyzed BA to form three-dimensional networks within the PVA structure through the formation of B–O–C crosslinks, which can be significantly enhanced by HCl.<sup>27,28</sup> The dominant crosslinking interactions between BA and PVA are hydrogen bonds, and they can be converted into covalent bonds by thermal treatment (annealing) or the addition of HCl catalyst, as identified in peak shift in the B–O–H linkage (from 659 cm<sup>–1</sup> in KP-PB to 663 cm<sup>–1</sup> in



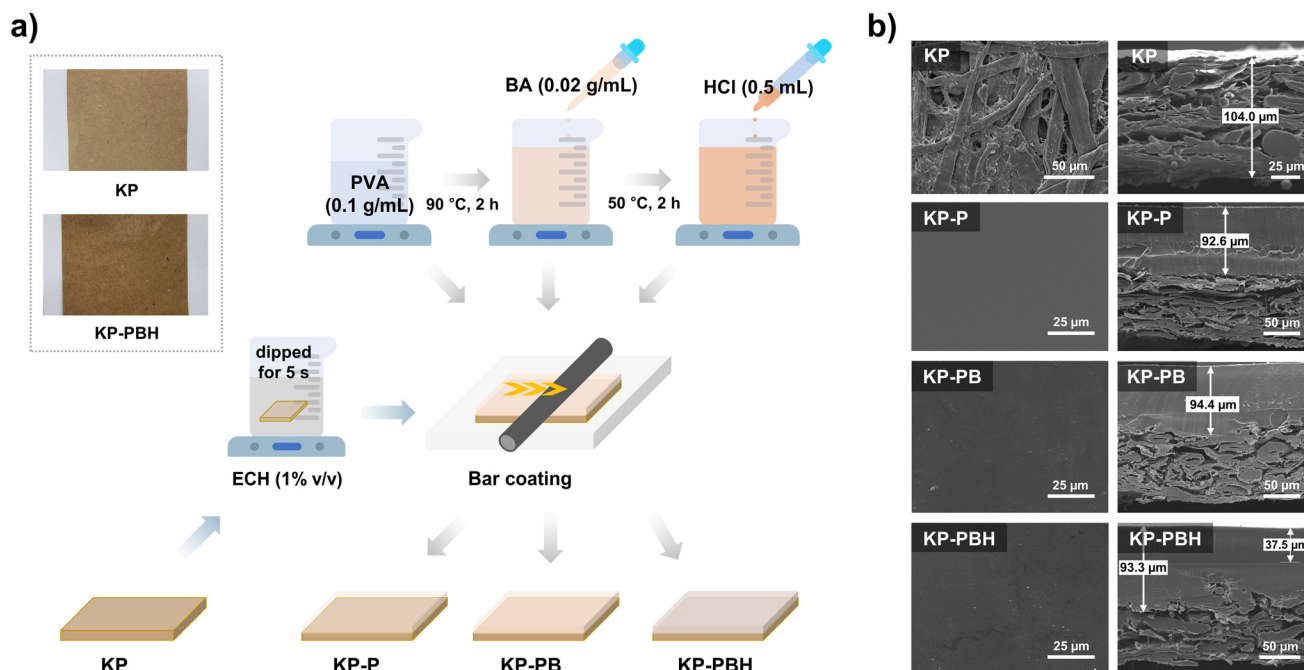


**Fig. 1** (a) Photos of KP and KP-PBH and the fabrication process of coated papers (KP-P, KP-PB, and KP-PBH). (b) SEM images of top-view and cross-section of coated papers. Scale bars are at the bottom right of each image.

**Table 1** Sample code and compositions of coated papers (KP-P, KP-PB, KP-PBH)

Sample	Composition						
	Paper			Coating layer			
	Kraft paper (%)	Epichlorohydrin (%)	NaOH (mL)	PVA (g)	BA (g)	HCl (mL)	Water (mL)
KP	100	0	0	0	0	0	0
KP-P	99	1	1	10	0	0	125
KP-PB	99	1	1	10	0.5	0	125
KP-PBH	99	1	1	10	0.5	0.5	125

KP-PBH).<sup>27</sup> The covalent crosslinking bonds from reaction between the epoxy group of ECH and the hydroxyl groups of cellulose fibers may be attributed to the peaks in carbonyl group at  $1710\text{ cm}^{-1}$ , which imparted structural stability to coated papers (Fig. 2c and d).

### Oxygen, water vapor barrier properties and oil resistance

The multiple crosslinks in coated papers (*i.e.*, hydrogen bond, borate ester, and ECH linkage) significantly enhance oxygen, water vapor barrier properties and oil resistance of KP (Fig. 3 and Table S1†). The barrier properties of pristine KP are not measurable due to its extreme weakness in moisture and oxygen, as the transmission rates exceeded the monitoring ranges of the devices for oxygen ( $1.0 \times 10^3\text{ cc m}^{-2}\text{ d}^{-1}$ ) and water vapor ( $4.32 \times 10^5\text{ g m}^{-2}\text{ d}^{-1}$ ) (Fig. 3a). The oxygen and water vapor transmission rates of KP-P and KP-PB are  $5.30 \pm 0.50$ ,  $1.92 \pm 0.04\text{ cc m}^{-2}\text{ d}^{-1}$  and  $50.67 \pm 4.04$ ,  $28.00 \pm 3.61\text{ g m}^{-2}\text{ d}^{-1}$ , respectively. The barrier properties are further increased in KP-PBH, exhibiting the lowest permeability to

oxygen ( $0.89 \pm 0.03\text{ cc m}^{-2}\text{ d}^{-1}$ ) and water vapor ( $5.17 \pm 0.35\text{ g m}^{-2}\text{ d}^{-1}$ ). This indicates that the barrier of the PVA coating is gradually enhanced by increasing crosslinking density in the coating layer with the incorporation of BA crosslinker and HCl catalyst. We note that these trends in barrier properties correspond to the results of BA-crosslinked PVA film analyzed in our previous report,<sup>27</sup> yet it is notable that these outstanding barrier properties are retained when the BA-crosslinked PVA is coated onto KP with ECH.

Oil resistance is also crucial for grease-containing products such as foods. The oil resistance was assessed by the kit test based on TAPPI T 559 protocol.<sup>45</sup> Kit solutions were prepared with different amounts of castor oil, *n*-heptane, and toluene to produce varying surface tension and viscosity levels. Reagent number 12 was regarded as the most aggressive oil. The oil resistance grade of pristine KP was rated as 1, and it was significantly elevated to 12 for KP-P, KP-PB, and KP-PBH. The notable improvement in oil resistance can be rationalized by two factors: (1) ECH treatment to KP may facilitate the for-



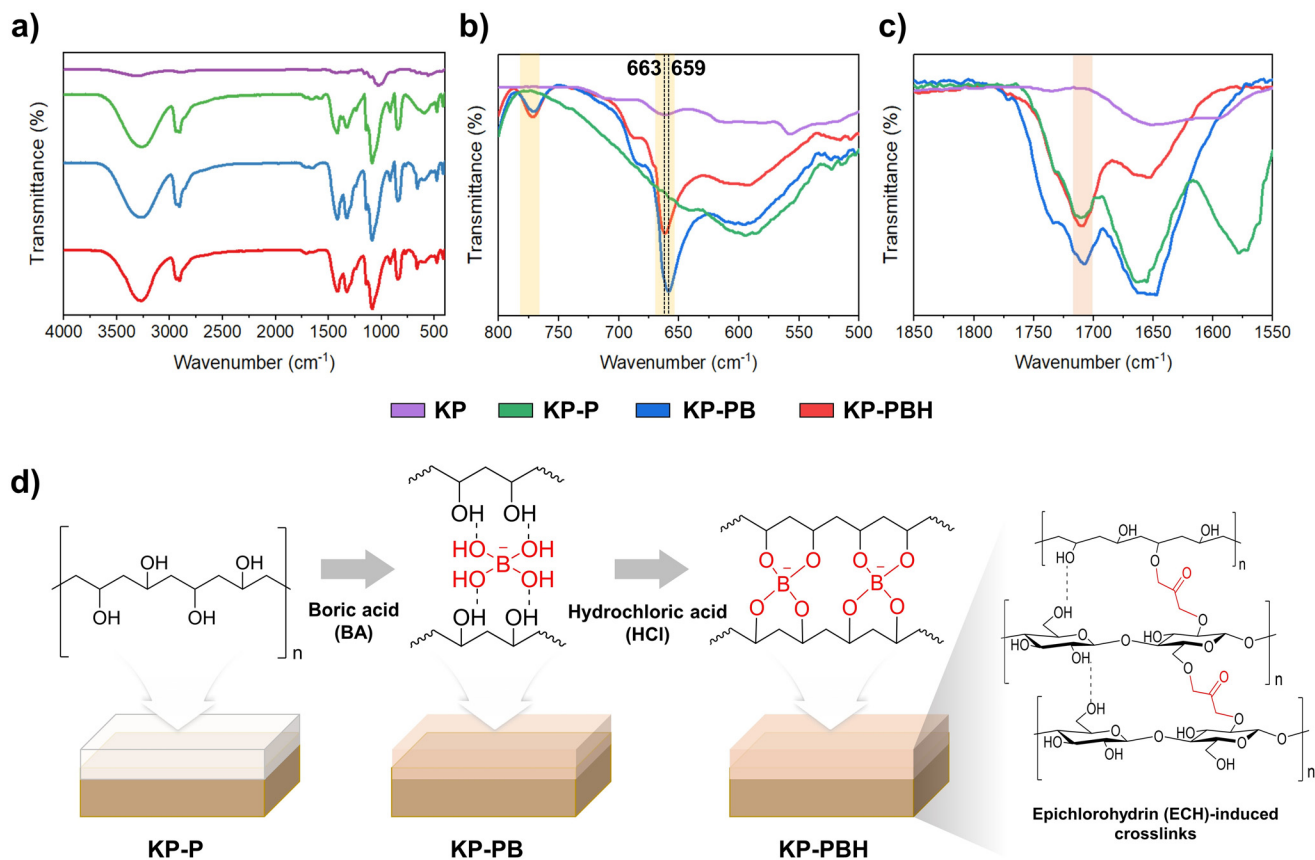


**Fig. 2** (a–c) FT-IR curves of KP and coated papers (KP-P, KP-PB, and KP-PBH). (b) The methaboric acid vibration at  $770\text{ cm}^{-1}$  and  $\text{BO}_3$  symmetric deformation vibration at  $659\text{--}663\text{ cm}^{-1}$  are indicated in yellow-shaded regions, respectively. Dashed lines represent the band shift within the range of B–O–H bond region. (c) The peaks of carbonyl group induced by ECH are marked in an orange-shaded region. (d) Chemical structure of coated papers. Crosslinking bonds (*i.e.*, hydrogen, borate ester, and ECH linkage bonds) are highlighted in red.

mation of a uniform and dense layer of cellulosic fibers, and (2) PVA coating solutions efficiently fill the porous structure of KP.

### Mechanical properties

The mechanical characterization reveals that the coated papers are mechanically robust (Fig. 3c and Table S1†). In dry condition (0% RH), while the tensile strength of KP is  $31.4 \pm 3.2$  MPa, the introduction of pristine PVA coating enhances the rigidity in KP-P ( $40.3 \pm 2.1$  MPa). The borate ester crosslinks in the PVA coating further improve the tensile strength, where KP-PB and KP-PBH show  $45.1 \pm 1.7$  and  $53.0 \pm 4.8$  MPa of tensile strength, respectively. KP-PBH also exhibits the highest fracture load ( $462.6 \pm 42.2$  kPa) than KP, KP-P, and KP-PB ( $199.4 \pm 3.1$ ,  $319.7 \pm 12.7$ ,  $361.8 \pm 10.1$  kPa, respectively). This is attributable to the strong intermolecular crosslinking bonds among the PVA chains and covalent crosslinks between cellulosic fibers and PVA.

The utility of both PVA and paper is highly constrained in wet conditions and moisture-sensitive areas since they are susceptible to damage by water vapor.<sup>46,47</sup> Remarkably, KP-PBH maintained high tensile strength ( $51.9 \pm 1.2$  MPa) when the samples were conditioned in 80% RH for 24 h (Fig. 3d).

Tensile strength of KP-PBH decreased merely 2.1% from dry to moist conditions, while KP, KP-P, and KP-PB showed 16.9, 40.0, and 14.0% reduction, respectively. We have previously reported that the HCl catalyst decreases the water solubility of BA-crosslinked PVA film from 100 to 55 wt%.<sup>27</sup> The increased crosslinking density in KP-PBH can bring about more compact polymer chains and decreased chain mobility, enhancing intermolecular force, and thus elevating material robustness and barrier properties.

### Biodegradation test simulating marine environment

Biodegradation test was performed by simulating marine environment per ASTM D6691-17<sup>48</sup> for 111 d to investigate whether the applied chemical modification to PVA coating (*i.e.*, the addition of BA, HCl, and ECH) hinders the biodegradation behavior of coated papers (KP-P, KP-PB, and KP-PBH). The carbon mineralization into  $\text{CO}_2$  of samples was monitored employing a systematically designed respirometer and using eulittoral seawater and sediment as inoculum (Fig. S1 and S2†). The coated papers exhibited significant biodegradation levels (59.8–81.6%, Fig. 4 and Table S2†).

The pristine KP, primarily consists of cellulose, showed rapid biodegradation ( $94.4 \pm 14.4\%$ ) as cellulose is readily



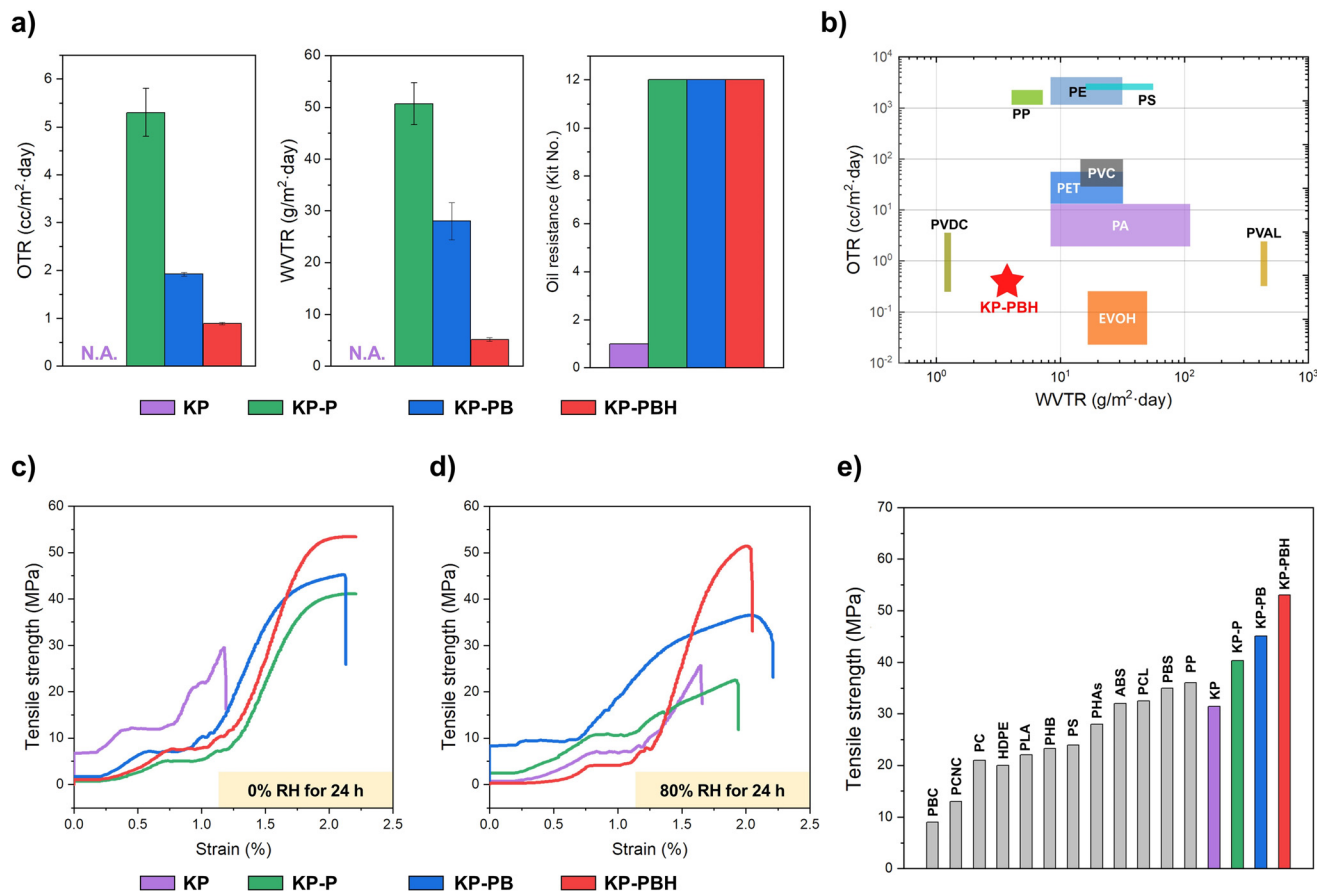


**Fig. 3** (a) Oxygen transmission rate (OTR), water vapor transmission rate (WVTR), and oil resistance of KP and coated papers (KP-P, KP-PB, and KP-PBH). (b) Comparative barrier properties of KP-PBH. (c and d) Tensile curves tested under dry and moist conditions. (e) Comparative tensile strength of commodity plastics and the coated papers. N.A.: not applicable.

hydrolyzed and assimilated by microorganisms.<sup>49,50</sup> KP-P exhibited notable biodegradation ( $81.6 \pm 17.0\%$ ), suggesting that the pristine PVA coating does not impede the biodegradation. The slower biodegradation of KP-P than KP is attributable to the ECH-induced crosslinks between PVA and cellulosic fibers. The chemical modification in PVA coating moderately dampened biodegradation of the coated papers. KP-PB showed slower biodegradation ( $59.2 \pm 27.7\%$ ) than KP-P. This can be rationalized by intermolecular borate ester crosslinks in KP-PB. On the other hand, KP-PBH exhibited biodegradation ( $60.5 \pm 18.4\%$ ) akin to KP-PB. We hypothesize that the chemical transition in dominant crosslinking bonds from hydrogen to covalent bonds does not significantly damage the biodegradability of coated papers. Although the covalent bonds are stronger than hydrogen bonds due to the share of electrons between atoms, the increased crosslinking units in the PVA matrix of KP-PBH may be attributed to the reduction in crystallinity, which can facilitate the biodegradation of polymers.<sup>27,51</sup>

After 111 d of the biodegradation test, the samples were centrifuged and analyzed with FT-IR (Fig. S3†). The characteristic bonds of PVA (e.g., wagging vibration of  $-\text{CH}$  at  $1416 \text{ cm}^{-1}$

and  $-\text{CH}$  stretching vibration at  $2908 \text{ cm}^{-1}$ ) are significantly decreased after biodegradation, suggesting the degradation of PVA (Fig. S3a–d†).<sup>52,53</sup> Interestingly, the symmetric deformation vibration of  $\text{BO}_3$  observed at  $661 \text{ cm}^{-1}$  in BA-crosslinked PVA (KP-PB and KP-PBH) was drastically reduced after biodegradation, indicating the degradation of crosslinks (Fig. S3e and f†). This implies that although the borate ester crosslinks significantly improve the oxygen and water vapor barrier properties and mechanical strength of coated papers, they do not significantly impact biodegradation behavior.

In the biodegradation test, where the bioreactors were continuously shaken at 180 rpm, PVA coating was detached from KP after 10 d of incubation. A hydrogel-like substance was attached to the aeration hose in the KP-PBH containing bioreactor (Fig. 5a). Subsequently, both KP and PVA hydrogel were disintegrated after 60 d of incubation (Fig. 5b). On the contrary, KP-PBH was not significantly disintegrated even after 300 d of incubation in the microcosm experiment, where KP-PBH was under the quiescent conditions (i.e., without mechanical stress, Fig. 5c). This indicates that effective disintegration of coated papers requires a synergy of both biotic (e.g., surface colonization and excretion of depolymerases) and



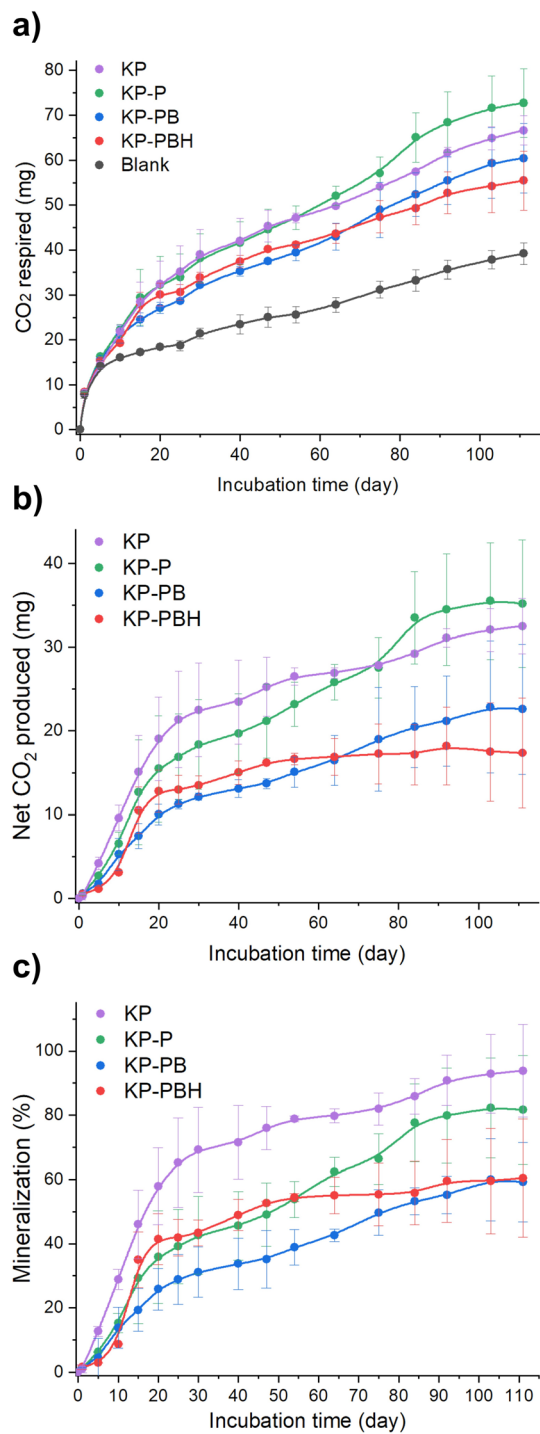


**Fig. 4** Results of biodegradation test simulating marine environment employing respirometer. (a) Cumulative respired CO<sub>2</sub>, (b) net CO<sub>2</sub> produced, and (c) mineralization of KP, KP-P, KP-PB, and KP-PBH, calculated based on the difference in CO<sub>2</sub> production between the samples and the blank (incubated without substrate) divided by theoretical CO<sub>2</sub> production. Error bars are standard deviations of cumulative values ( $n = 2$ ). The detailed description for calculation is in Text S1.†

abiotic degradation (e.g., mechanical and photodegradation). This result suggests that coated papers can be degraded in the ocean by mechanical forces such as ocean tides and waves,

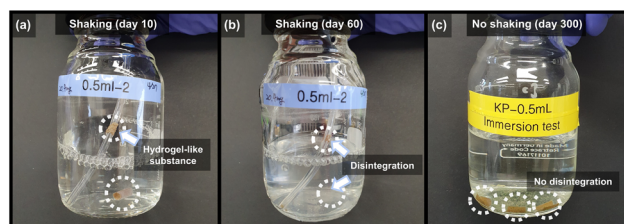


**Fig. 5** Photos of KP-PBH bioreactor showing the impact of mechanical stress on disintegration. KP-PBH after (a) 10 d and (b) 60 d of the biodegradation test using a respirometer where the bioreactors were shaken at 180 rpm. (c) KP-PBH after 300 d of immersion in the marine seawater and sediment mixture (i.e., no shaking).

minimizing the harm to marine animal suffocation and entanglement.

Microorganisms that colonized the surface of coated papers were investigated after 60 d of the microcosm experiment. The SEM images corroborate the surface colonization and degradation of coated papers by diverse unicellular organisms (Fig. 6). Intertwined fungal hypha extensively colonized the surface of the PVA.<sup>54,55</sup> Spiral and rod cells (*ca.* 1–2  $\mu\text{m}$ -sized) are the main morphotypes of observed bacteria. Particularly intriguing are the curved-rod cells “assimilating” the PVA coating of KP-PBH, which unequivocally evidence the biodegradability of BA-crosslinked PVA coating by marine bacteria (Fig. 6l). The spiral-, rod-, and curved-rod-shaped bacteria also extensively attached to the surface on cellulose fiber in uncoated side, suggesting that the PVA matrix and KP undergo biodegradation simultaneously (Fig. 6g–j). In addition, the pitting and fissures found in the residues collected at the end of the biodegradation test (111 d) further support the degradation of BA-crosslinked PVA coating (Fig. S4†).

Together, our findings from the biodegradation test, molecular structure change, surface degradation by marine microorganisms, and the effect of mechanical stress demonstrate that the coated papers would be effectively disintegrated and eventually mineralized by diverse marine microorganisms. The plausible end-of-life scenario of coated papers in case of leakage in the marine environment is graphically envisioned (Fig. 7).

### Biocompatibility tests

KP and PVA are widely recognized as biocompatible polymers utilized for food packaging and biomedical applications, respectively.<sup>14,52,56</sup> For *in vitro* biocompatibility tests, the coated papers (KP-P, KP-PB, KP-PBH) were added to the Dulbecco's modified Eagle's medium in two concentrations (0.05 and 0.2  $\text{mg mL}^{-1}$ , denoted as low and high, respectively), where MEF and HEK293 cells are cultured. After 48 h of incubation, the cell viability was measured *via* Annexin-V staining and flow analysis. While starving cells for 24 h increased Annexin-V+ apoptotic cells ( $36.3 \pm 5.0\%$  in MEFs and  $17.1 \pm 1.8\%$  in HEK293 cells), the ratio of apoptotic cells in sample treated groups was similar to control samples (Fig. 8a and



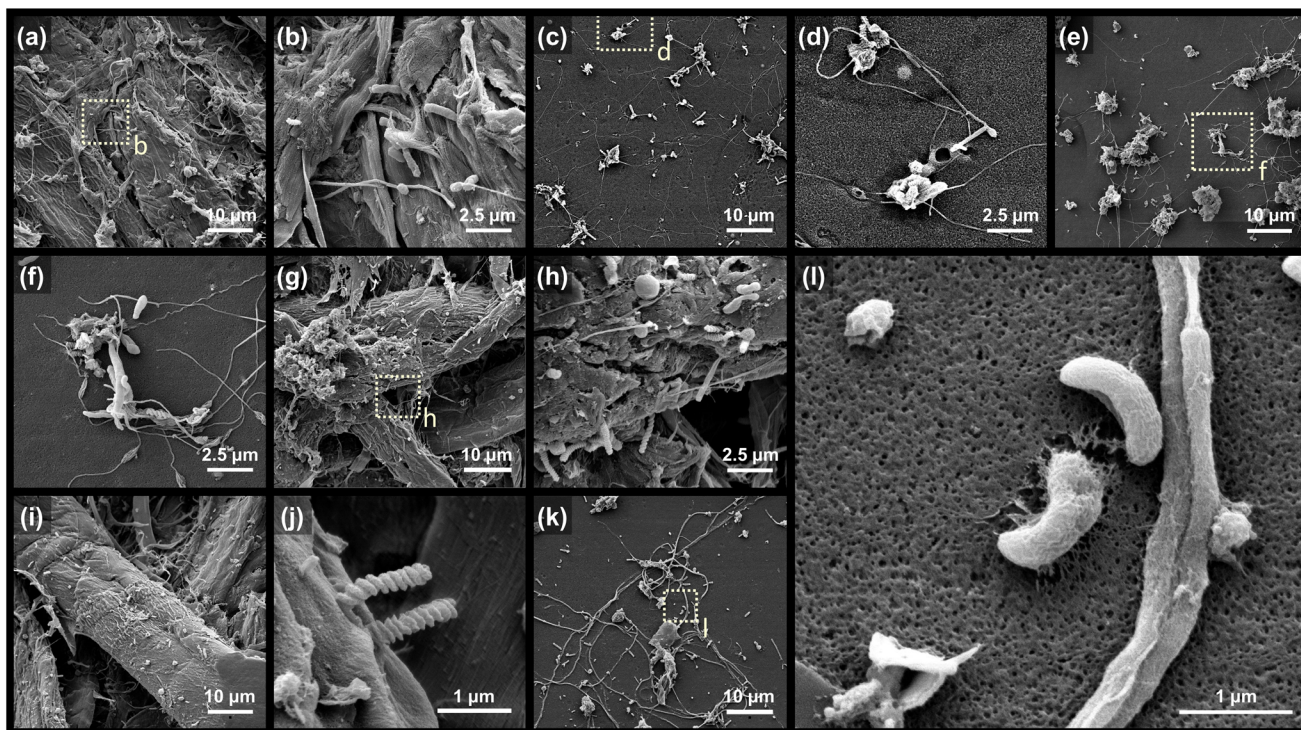


**Fig. 6** SEM images of surface morphology and microbes. (a and b) KP, (c and d) KP-P, (e and f) KP-PB, (g and h) KP-PB (uncoated side), (i and j) KP-PBH (uncoated side), and (k and l) KP-PBH after being immersed in seawater and sediment mixture for 60 d. The curved-rod bacteria assimilating the BA-crosslinked PVA coating are highlighted in (l). Dotted square region indicates the enlargement in the subsequent image. Scale bars are located at the bottom right of each image.

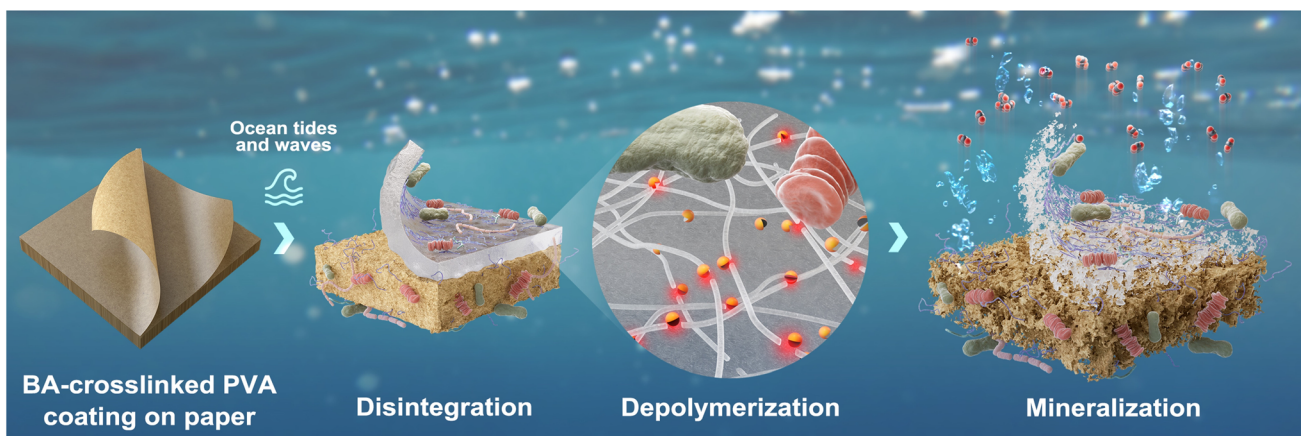


**Fig. 7** Proposed end-of-life scenario of papers coated by BA-crosslinked PVA in the marine environment. The coated papers potentially be disintegrated by marine microorganisms and ocean waves and tides. The depolymerization of PVA coating and paper is then mediated by extracellular depolymerases such as oxidases and cellulases, after which the small subunits (oligomers and monomers) are assimilated by microbial cells. The carbon components in the coated papers are ultimately mineralized into  $\text{CO}_2$ , posing no harm in the ocean.

$\text{S}5^+$ ). Namely, when MEF and HEK293 cells were cultivated with low ( $0.05 \text{ mg mL}^{-1}$ ) and high ( $0.2 \text{ mg mL}^{-1}$ ) concentrations of coated papers, the cell viabilities were all higher than 95%. The apoptotic cell rates of KP-PBH-treated samples ( $0.04 \pm 0.08\%$  for MEF and  $0.45 \pm 0.05\%$  for HEK293 cells in  $0.2 \text{ mg mL}^{-1}$ , respectively) were lower than that of KP, KP-P, and KP-PB.

For *in vivo* biocompatibility test, the coated papers were dissolved in drinking water at  $0.3 \text{ mg mL}^{-1}$  and provided to 6-week-old mice for 30 d. To test if the intake of coated papers causes health issues, vital organs such as the heart, lungs, kidney, liver, and spleen were examined by histological analyses. Hematoxylin and eosin (H&E) staining suggests that overall tissue architectures, immune cell infiltration, and extra-



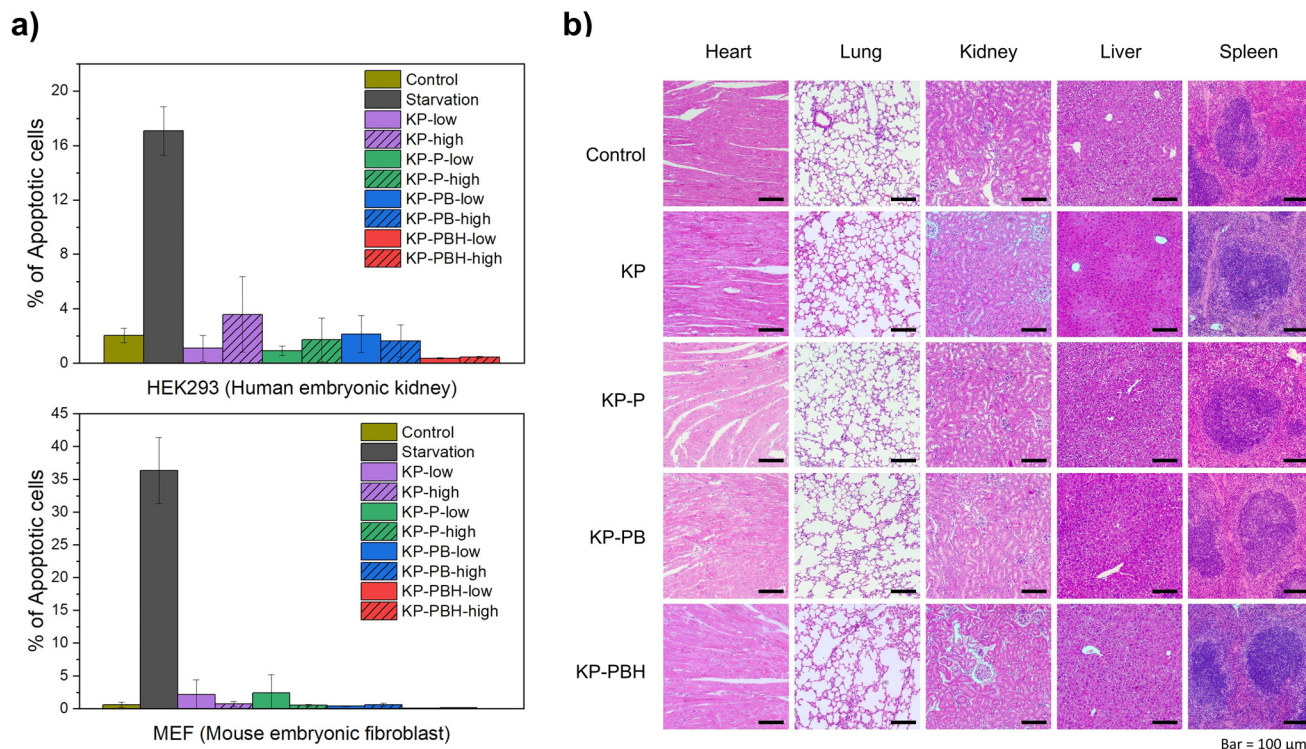


**Fig. 8** Biocompatibility test results. The apoptotic cell rates of (a) Human embryonic kidney (HEK293) and mouse embryonic fibroblast (MEF) cells from *in vitro* biocompatibility tests. Error bars indicate standard deviations ( $n = 3$ ). (b) Histological images of heart, lung, kidney, liver, and spleen from *in vivo* biocompatibility test with 6-week-old mice for 30 d. Scale bars are located at the bottom right of the images.

cellular matrix appearance were not changed (Fig. 8b). No tissue hemorrhage, as well as fibrosis, was observed in all samples, suggesting that the coated papers are highly biocompatible *in vivo*. The results indicate that incorporation of BA, HCl, and ECH into PVA coating on KP does not lead to increased toxicity. Therefore, the coated papers may not threaten marine fauna even in the case of unintentional leakage to nature environment.

### Sustainable implications

The widespread accumulation of plastic materials such as single-use packages and their detrimental impacts on ecosystems highlight the urgent need for biodegradable alternatives. Nonetheless, developing biodegradable packaging materials is often challenging due to the trade-off between performance and sustainability.<sup>38</sup> This work demonstrates a successful breakthrough in addressing the dilemma by balancing material performance and environmental soundness, marking a green advance in sustainable packaging.<sup>57</sup>

The barrier properties and mechanical robustness of BA-crosslinked PVA coated papers exceed those of commodity plastics used for packaging applications such as HDPE and PLA (Fig. 3, S6 and Table S3<sup>†</sup>). In addition, BA-crosslinked PVA has unequivocal environmental merit compared to non-degradable coating materials, including PE, PP, and EVOH.

We address the crucial consideration of the end-of-life scenario of packaging material, contributing to an informed choice

of sustainable materials in the market.<sup>13,19</sup> In particular, the focus on marine environments distinguishes this study, given that many biodegradable plastics exhibit limited biodegradation in marine settings, including PLA and PBAT.<sup>32,34,49,58</sup> Only a few biodegradable plastics, such as polyhydroxybutyrate, polycaprolactone, cellulose diacetate, and PVA are known to biodegrade in the marine environment within a reasonable time frame (*i.e.*, months to years).<sup>59,60</sup> The coated papers exhibited remarkable mineralization levels (59.2–81.6% over 111 d) in the simulated marine environment, suggesting that the products have a low impact on the environment, even compared to biodegradable plastics.<sup>49</sup> Furthermore, we assessed biodegradation based on the respiratory activity of microorganisms, rather than relying on weight loss. Weight loss measurement can overlook the generation of micro- and nanoplastics.<sup>55</sup> We quantitatively assessed the carbon mineralization into CO<sub>2</sub> of coated papers using a respirometer, ensuring their complete end-of-life in the natural environment. On the other hand, we reveal that the coated papers are biocompatible *in vitro* and *in vivo*. In our recent report, varying concentrations of ECH (0–3%) on KP-PBH did not induce any phytotoxic impact on the germination of ryegrass (*Lolium multiflorum*) seeds.<sup>61</sup>

While we demonstrate the remarkable biodegradation behavior of the coated papers in the marine environment, it is crucial to quantitatively analyze their low environmental footprint during the manufacturing process. The *E* factor (environ-



mental factor), a widely adopted green metric for decades, represents the mass ratio of total waste to the desired product.<sup>62,63</sup> We calculated the *E* factor using the mass of chemicals used in the fabrication of KP-PBH (see Text S2† for detailed calculation). Assuming that 90% of chemicals (*i.e.*, BA, HCl, and ECH solutions) are recycled, the resulting *E* factor is 0.17. This indicates that the fabrication process of KP-PBH is environmentally efficient.<sup>64</sup> We hypothesize that the *E* factor of coated papers reaches a minimum on a larger scale, as the applied chemicals are readily recycled. However, a thorough assessment of waste during the fabrication process, including any unused coating materials or other solvents, is a prerequisite for further analysis.<sup>62,63,65</sup>

Further examination is warranted, including (1) the holistic life-cycle assessment, (2) the applicability of BA-crosslinked PVA coatings to other types of papers such as paperboard and recycled paper, (3) a comparison of BA-crosslinked coated paper with papers coated by PE and EVOH, and (4) meticulous estimation of the *E* factor in a scaled-up process, which will be pursued in future researches.

## Conclusions

We present BA-crosslinked PVA as a high-performance and sustainable paper coating material. The PVA solutions were prepared with different compositions by adding BA and HCl and coated on KP with ECH *via* a facile method. The incorporation of BA to PVA forms borate ester crosslinking bonds among PVA chains, which is intensified by the HCl catalyst. The ECH added as a coating binder induces covalent crosslinks between the epoxy group of ECH and the hydroxyl groups of PVA, which imparts structural stability to coated papers (KP-P, KP-PB, KP-PBH). BA-crosslinked PVA coating can largely complement the major drawback of paper, the susceptibility to water and oxygen, and poor mechanical strength. The coated papers exhibit outstanding oxygen ( $\sim 0.89$  cc m<sup>-2</sup> d<sup>-1</sup>) and water vapor barrier ( $\sim 5.17$  g m<sup>-2</sup> d<sup>-1</sup>) properties as well as oil resistance (grade 12 in kit test), tensile strength ( $\sim 53.0$  MPa), and fracture load ( $\sim 462.6$  kPa). The tensile strength of KP-PBH is maintained even in moist conditions (51.9 MPa, 80% RH).

We examined the biodegradation behavior of coated papers in the simulated marine environment employing respirometer. The coated papers were significantly mineralized into CO<sub>2</sub> (59.8–81.6%) over 111 d in the biodegradation test. The SEM images evidence surface colonization and degradation of coated papers by diverse marine fungi and bacteria. In addition, the mechanical stress (*i.e.*, shaking of bioreactors) triggered the detachment of the PVA coating from the KP and subsequent disintegration. The *in vitro* biocompatibility tests using HEK 293 and MEF cells suggest that the coated papers have negligible cytotoxicity. The *in vivo* biocompatibility test conducted by feeding sample-dissolved drinking water to mice for 30 d showed that the intake of coated papers has no adverse effect on vital organs. Consequently, BA-crosslinked PVA coating on paper is an environmentally benign strategy

that can enhance the performance of paper packaging while retaining environmental sustainability.

## Experimental

### Materials and reagents

Poly(vinyl alcohol) (PVA) resins (degree of hydrolysis: 98.0–99.5%, molecular weight: 74 800 g mol<sup>-1</sup>) were supplied by OCI Co. Ltd. (Incheon, South Korea). Boric acid (BA), (±)-epi-chlorohydrin (ECH), hydrogen chloride (37 wt%, HCl), glutaraldehyde, ethanol, osmium tetroxide (4 wt%), KH<sub>2</sub>PO<sub>4</sub>, NH<sub>4</sub>Cl, and Ba(OH)<sub>2</sub> were purchased from Sigma Aldrich Chemical Co. (St Louis, MO, USA). 3-Methyl acetate was obtained from Junsei (Tokyo, Japan). Dulbecco's modified Eagle's medium (DMEM) (1×), Penicillin–streptomycin solutions (100×), and Dulbecco's phosphate-buffered saline (D-PBS) (1×) were purchased from Welgene, Inc. (Gyeongsan-si, South Korea). Paraformaldehyde (PFA) (8% w/v), and fetal bovine serum were obtained from Thermo Fisher Scientific (MA, USA). Mayer's hematoxylin and eosin (H&E) solutions were purchased from Cancer Diagnostics, Inc. (Manassas, VA, USA). All chemicals were used as received.

### Preparation of Kraft paper coated by BA-crosslinked PVA

Initially, 10 g of PVA was dissolved in 100 mL of distilled water and agitated at 90 °C and 350 rpm for 2 h. BA (0.5 g) was dissolved in 25 mL of distilled water at 40 °C for 10 min. The BA solution was introduced in a dropwise manner to the PVA solution stirring for 2 h. HCl (0.5 mL) was subsequently added dropwise to the PVA-BA solution stirring at 50 °C for 10 min.<sup>27</sup> Subsequently, KP was dipped in the 1% v/v ECH aqueous solution for 5 s and utilized as substrate.<sup>61</sup> The BA-crosslinked PVA solutions were coated onto the ECH-treated KP *via* bar-type automatic film coating apparatus (KIPAE E&T Co. Ltd., South Korea) and dried at 25 °C for 12 h. The coated papers were placed in a 25 °C oven for 24 h to induce crosslinking between components.

The thickness of the coating layer was controlled at around 90 μm to investigate varying physicochemical properties as well as biodegradability and biocompatibility dependent on different coating compositions. The resulting samples are denoted as KP-x, where x indicates the type of PVA coating. KP-P is paper coated by pristine PVA. KP-PBH and KP-PB are the papers coated by BA-crosslinked PVA with or without the HCl catalyst, respectively (Table 1).

### Fourier-transform infrared spectroscopy (FT-IR)

The chemical bonds were characterized by Fourier-transform infrared spectroscopy (FT-IR) recorded on a Spectrum 65 FTIR spectrometer (PerkinElmer Co. Ltd., MA, USA) from 4000 to 400 cm<sup>-1</sup> in the attenuated total reflection (ATR) mode at a scan speed of 64 cm s<sup>-1</sup>.



### Barrier properties

The oxygen transmission rate (OTR) was measured *via* an OTR 8101e oxygen permeation analyzer (Systech Instruments Co. Ltd., IL, USA) per ASTM D3985 at 23 °C and 0% relative humidity (RH). The water vapor transmission rate (WVTR) was evaluated using a WVTR 7001 (Systech Instruments Co. Ltd., IL, USA) per ASTM F1249 at 23 °C and 90% RH. The results of barrier properties were averages of 3 respective measurements.

The oil resistance of the coated papers was determined based on the TAPPI T 559 protocol (*i.e.*, kit test). Kit solutions were prepared with different amounts of castor oil, *n*-heptane, and toluene to produce varying surface tension and viscosity levels. Reagent number 12 was regarded as the most aggressive oil, and the oil resistance was determined as an average of 5 respective measurements.

### Mechanical characterization

Mechanical properties were characterized by tensile and bursting strength tests. The tensile specimens were cut into dumb-bell-shape in accordance with ASTM D638-03 type IV and tested using a universal testing machine QM100T-C (Qmesys Co. South Korea) at a head travel rate of 200 mm min<sup>-1</sup> in two conditions: (1) dried at 0% RH for 24 h, (2) conditioned under 80% RH for 24 h prior to the test to assess the tensile strength in moist conditions. The results were averages of at least 5 respective measurements.

The bursting strength was performed using a digital burst strength test machine SJTM-003 (Sejin Technology Co., Ltd, South Korea) based on ISO 2759. The samples were cut into even-edged 100 × 100 mm specimens through an experimental cutter blade. The test was conducted at a pump speed of 170 ± 15 mL min<sup>-1</sup>, and the clamp pump was set at 250 kPa. The test was performed 10 times for each specimen under controlled conditions of 23 °C and 50% RH.

### Scanning electron microscopy (SEM)

The samples were dried in a CO<sub>2</sub> atmosphere for 24 h and sputtered with gold-palladium alloy to be morphologically observed *via* JEOL-7800F (JEOL Ltd., Tokyo, Japan). In addition, the cut surface of coated papers was observed to evaluate the cross-sectional morphology at a magnification of 500×. In addition, microorganisms associated with the biodegradation of the coated papers were inspected (see details in Text S3†).

### Biodegradation test

The biodegradation of coated papers in the marine environment was evaluated per ASTM D6691-17<sup>48</sup> with some modifications. Since the density of the coated papers is higher than seawater, they may sink and interact with both eulittoral seawater and sediment in the case of leakage;<sup>66,67</sup> thus, coastal surface seawater and sediments from (1) Ganwoldo, Seosan and (2) Haeundae beach, Busan, South Korea were collected in sterile 1 L water sampling bottles in March 2022 (Fig. S1†).

The sampling bottles were immediately sealed and kept in the fridge (4 °C) until used as inoculum within 48 h.

The systematically designed respirometer was employed to assess the biodegradation based on the degree of carbon mineralization into CO<sub>2</sub>, as previously described (Fig. S2†).<sup>40</sup> The inoculum was vigorously shaken and filtered with a 40 μm cell strainer to prevent inclusion of solid particles, which was then supplemented with 0.5 g KH<sub>2</sub>PO<sub>4</sub> and 0.1 g NH<sub>4</sub>Cl per liter. One hundred mL of inoculum was mixed with 20.0–27.6 mg of KP and coated papers (1 × 1 cm) per bioreactor to ensure identical surface bioavailability of samples.<sup>60,68,69</sup> The biodegradation test was performed at 30 °C and the bioreactors were continuously shaken at 180 rpm to simulate ocean tides and waves. The bioreactor that only contains inoculum (*i.e.*, without polymer substrate) is denoted as blank.

In the respirometer, nitrogen gas (99.999%, World Energys, South Korea) was flushed into each bioreactor for 15 min to eject CO<sub>2</sub> in the headspace, and subsequently high-purity air (99.999%, World Energys, South Korea) was supplied. The air initially passed through 2 L of 50 mM Ba(OH)<sub>2</sub> to eliminate CO<sub>2</sub>. The air was then constantly pushed at 10 mL min<sup>-1</sup> into bioreactors to provide O<sub>2</sub> and to release respired CO<sub>2</sub> throughout the entire biodegradation period.<sup>70</sup> The respired CO<sub>2</sub> from each bioreactor was quantitatively assessed using titration method (see Text S1† for detailed calculation).<sup>40</sup> The biodegradation test was performed for 111 d in biological duplicate. After the biodegradation test, the samples were centrifuged at 4000 rpm for 10 min and further analyzed through FT-IR and SEM.

### Microcosm experiment

The microcosm test was conducted to observe surface colonization by marine microorganisms *via* SEM and investigate the effect of mechanical stress on the degradation. KP-PBH strips (1 × 1 cm) were immersed in the same inoculum (seawater and sediment used in the biodegradation test) at 25 °C for 300 d without intensive oxygen supply and shaking of bioreactor.

### *In vitro* biocompatibility tests

The human embryonic kidney (HEK293) and mouse embryonic fibroblast (MEF) cell lines were purchased from ATCC (Manassas, VA, USA). The cells were grown in DMEM supplemented with 10% fetal bovine serum and 1% penicillin-streptomycin at 37 °C in a humidified incubator with 7.5% CO<sub>2</sub>. The samples were minced manually and dissolved in de-ionized water at 200 °C for 24 h and diluted to 0.5 and 2 mg mL<sup>-1</sup>. The samples were autoclaved, diluted 10-fold, and added to the cell culture media in 12-well plates (*i.e.*, the substrate concentrations were 0.05 and 0.2 mg mL<sup>-1</sup> and denoted as low and high, respectively). After 48 h, the viability of starved, treated, and control cells was assessed by Dead Cell Apoptosis Kits with Annexin V Alexa Fluor 488 & Propidium Iodide (PI) (Thermo Fisher Scientific, MA, USA) following the manufacturer's instruction. Briefly, the cells were trypsinized, washed with ice-cold PBS, and resuspended with 1× annexin-binding buffer. To distinguish live and dead cells, Alexa Fluor



488 Annexin V and PI working solution was added and incubated at room temperature for 15 min. After adding 1× annexin-binding buffer, flow cytometry analyses were performed using a Sony LE-SH800s FACS (SONY, Tokyo, Japan). Annexin+ and PI− apoptotic cells were quantified. All tests were conducted in triplicate.

### **In vivo biocompatibility test**

All animal procedures were performed in accordance with the Guidelines for Care and Use of Laboratory Animals of Korea Advanced Institute of Science and Technology (KAIST) and approved by the Institutional Animal Care and Use Committee (IACUC) of KAIST (approval number: KA2023-033-v1). Six-week-old male C57BL/6J mice were purchased from KAIST Laboratory Animal Resource Center (Daejeon, South Korea) and maintained in a specific pathogen-free condition. The coated paper strips were minced, dissolved in drinking water at 0.3 mg mL<sup>−1</sup> and autoclaved. Mice were fed sample-containing sterilized water for 30 d *ad libitum*. The sample containing drinking water was changed every week. Control group mice were fed with normal drinking water. After 30 d, mice were euthanized by CO<sub>2</sub> inhalation, and the heart, lungs, liver, spleen, and kidney were collected. The collected tissues were washed in PBS and fixed in 4% PFA at 4 °C overnight. Then, to remove residual PFA from the tissues, PBS washes were performed for 2 d. The tissues were processed for histological analyses and embedded in a paraffin block, sliced, and then stained by hematoxylin and eosin (H&E) solutions. The experiment was conducted in triplicate.

## Conflicts of interest

There are no conflicts to declare.

## Acknowledgements

This work was supported by the Hyundai Motor Chung Mong-Koo Foundation, National Research Foundation of Korea (NRF) grant funded by the Korea government (MSIT) (2022R1A4A3029607, 2022R1F1A1064064, and RS-2023-00209472), and Korea Institute of Planning and Evaluation for Technology in Food, Agriculture and Forestry (IPET) through Livestock Industrialization Technology Development Program, funded by Ministry of Agriculture, Food and Rural Affairs (MAFRA)(321089-5). This research was also part of a project titled 'Development of 1 tonf-class Ultrasonic Pretreatment-Pyrolysis Liquefaction Facility and Operating System for Marine Plastic Recycling' funded by the Ministry of Oceans and Fisheries, Korea (20200104).

## References

- 1 A. Cózar, F. Echevarría, J. I. González-Gordillo, X. Irigoien, B. Úbeda, S. Hernández-León, Á. T. Palma, S. Navarro, J. García-de-Lomas and A. Ruiz, *Proc. Natl. Acad. Sci. U. S. A.*, 2014, **111**, 10239–10244.
- 2 S. B. Borrelle, J. Ringma, K. L. Law, C. C. Monnahan, L. Lebreton, A. McGivern, E. Murphy, J. Jambeck, G. H. Leonard and M. A. Hilleary, *Science*, 2020, **369**, 1515–1518.
- 3 R. Geyer, J. R. Jambeck and K. L. Law, *Sci. Adv.*, 2017, **3**, e1700782.
- 4 L. Lebreton, J. Van Der Zwet, J.-W. Damsteeg, B. Slat, A. Andrady and J. Reisser, *Nat. Commun.*, 2017, **8**, 1–10.
- 5 M. Cole, P. Lindeque, E. Fileman, C. Halsband, R. Goodhead, J. Moger and T. S. Galloway, *Environ. Sci. Technol.*, 2013, **47**, 6646–6655.
- 6 B. Li, W. Liang, Q.-X. Liu, S. Fu, C. Ma, Q. Chen, L. Su, N. J. Craig and H. Shi, *Environ. Sci. Technol.*, 2021, **55**, 10471–10479.
- 7 C. J. Thiele, M. D. Hudson, A. E. Russell, M. Saluveer and G. Sidaoui-Haddad, *Sci. Rep.*, 2021, **11**, 1–12.
- 8 K. R. Nicastro, R. L. Savio, C. D. McQuaid, P. Madeira, U. Valbusa, F. Azevedo, M. Casero, C. Lourenço and G. I. Zardi, *Mar. Pollut. Bull.*, 2018, **126**, 413–418.
- 9 F. Ribeiro, E. D. Okoffo, J. W. O'Brien, S. Fraissinet-Tachet, S. O'Brien, M. Gallen, S. Samanipour, S. Kaserzon, J. F. Mueller and T. Galloway, *Environ. Sci. Technol.*, 2020, **54**, 9408–9417.
- 10 X. Zhao and F. You, *Environ. Sci. Technol.*, 2022, **56**, 11780–11797.
- 11 UNEP, Single-Use Plastics: A Roadmap for Sustainability, 2018.
- 12 OECD, *Global Plastics Outlook*, 2022.
- 13 M. Mujtaba, J. Lipponen, M. Ojanen, S. Puttonen and H. Vaittinen, *Sci. Total Environ.*, 2022, **851**, 158328.
- 14 K. Khwaldia, E. Arab-Tehrany and S. Desobry, *Compr. Rev. Food Sci. Food Saf.*, 2010, **9**, 82–91.
- 15 H. Li, Y. Qi, Y. Zhao, J. Chi and S. Cheng, *Prog. Org. Coat.*, 2019, **135**, 213–227.
- 16 P. Tyagi, K. S. Salem, M. A. Hubbe and L. Pal, *Trends Food Sci. Technol.*, 2021, **115**, 461–485.
- 17 M. Imran, A.-M. Revol-Junelles, A. Martyn, E. A. Tehrany, M. Jacquot, M. Linder and S. Desobry, *Crit. Rev. Food Sci. Nutr.*, 2010, **50**, 799–821.
- 18 J. Wang, M. Euring, K. Ostendorf and K. Zhang, *J. Bioresour. Bioprod.*, 2022, **7**, 1–13.
- 19 S. RameshKumar, P. Shaiju and K. E. O'Connor, *Curr. Opin. Green Sustain. Chem.*, 2020, **21**, 75–81.
- 20 S. Lambert and M. Wagner, *Chem. Soc. Rev.*, 2017, **46**, 6855–6871.
- 21 Z. H. Qin, J. H. Mou, C. Y. H. Chao, S. S. Chopra, W. Daoud, S. Y. Leu, Z. Ning, C. Y. Tso, C. K. Chan and S. Tang, *ChemSusChem*, 2021, **14**, 4103–4114.
- 22 K. W. Meereboer, M. Misra and A. K. Mohanty, *Green Chem.*, 2020, **22**, 5519–5558.
- 23 Z. Zhou, T. Liu, Y. Tan, W. Zhou, Y. Wang, S. Q. Shi, S. Gong and J. Li, *Compos. Sci. Technol.*, 2023, 110130.
- 24 J. Tan, Q. Zhu, D. Li, N. Huang, Z. Wang, Z. Liu and Y. Cao, *Int. J. Biol. Macromol.*, 2023, **227**, 1305–1316.



- 25 P. Sun, S. Wang, Z. Huang, L. Zhang, F. Dong, X. Xu and H. Liu, *Green Chem.*, 2022, **24**, 7519–7530.
- 26 H. Eslami and T. H. Mekonnen, *Sustainable Mater. Technol.*, 2023, **37**, e00694.
- 27 K. Park, Y. Oh, P. K. Panda and J. Seo, *Prog. Org. Coat.*, 2022, **173**, 107186.
- 28 M. Lim, H. Kwon, D. Kim, J. Seo, H. Han and S. B. Khan, *Prog. Org. Coat.*, 2015, **85**, 68–75.
- 29 J. H. Woo, N. H. Kim, S. I. Kim, O.-K. Park and J. H. Lee, *Composites, Part B*, 2020, **199**, 108205.
- 30 C. Chen, Y. Chen, J. Xie, Z. Xu, Z. Tang, F. Yang and K. Fu, *Prog. Org. Coat.*, 2017, **112**, 66–74.
- 31 N. Wang, L. Zhao, C. Zhang and L. Li, *J. Appl. Polym. Sci.*, 2016, **133**, 43246.
- 32 S. Choe, Y. Kim, Y. Won and J. Myung, *Front. Chem.*, 2021, **9**, 671750.
- 33 N. Lucas, C. Bienaime, C. Belloy, M. Queneudec, F. Silvestre and J.-E. Nava-Saucedo, *Chemosphere*, 2008, **73**, 429–442.
- 34 T. P. Haider, C. Völker, J. Kramm, K. Landfester and F. R. Wurm, *Angew. Chem., Int. Ed.*, 2019, **58**, 50–62.
- 35 T. F. Nelson, R. Baumgartner, M. Jaggi, S. M. Bernasconi, G. Battagliarin, C. Sinkel, A. Künkel, H.-P. E. Kohler, K. McNeill and M. Sander, *Nat. Commun.*, 2022, **13**, 5691.
- 36 X.-F. Wei, M. S. Hedenqvist, L. Zhao, A. Barth and H. Yin, *Green Chem.*, 2022, **24**, 8742–8750.
- 37 F. Brilllet, M. Cregut, M. Durand, C. Sweetlove, J. Chenèble, J. l'Haridon and G. Thouand, *Green Chem.*, 2018, **20**, 1031–1041.
- 38 K. Ghosh and B. H. Jones, *ACS Sustain. Chem. Eng.*, 2021, **9**, 6170–6187.
- 39 X. Zhao, K. Cornish and Y. Vodovotz, *Environ. Sci. Technol.*, 2020, **54**, 4712–4732.
- 40 S. Choe, Y. Kim, G. Park, D. H. Lee, J. Park, A. T. Mossisa, S. Lee and J. Myung, *ACS Appl. Polym. Mater.*, 2022, **4**, 5077–5090.
- 41 B. D. James, C. P. Ward, M. E. Hahn, S. J. Thorpe and C. M. Reddy, *ACS Sustain. Chem. Eng.*, 2024, **12**, 1185–1194.
- 42 D. Mboowa, *Biomass Convers. Biorefin.*, 2021, **14**(1), 1–12.
- 43 H. Liu, H. Yano and K. Abe, *Cellulose*, 2023, **30**, 211–222.
- 44 I. Y. Prosanov, S. Abdulrahman, S. Thomas, N. Bulina and K. Gerasimov, *Mater. Today Commun.*, 2018, **14**, 77–81.
- 45 T. TAPPI, Grease resistance test for paper and paperboard, TAPPI Press, Atlanta, GA, USA, 2012.
- 46 X. Fang, Y. Qing, Y. Lou, X. Gao, H. Wang, X. Wang, Y. Li, Y. Qin and J. Sun, *ACS Mater. Lett.*, 2022, **4**, 1132–1138.
- 47 S. E. Selke, J. D. Culter, R. A. Auras and M. Rabnawaz, *Plastics packaging: properties, processing, applications, and regulations*, Carl Hanser Verlag GmbH Co KG, 2021.
- 48 ASTM D6691-17, Standard Test Method for Determining Aerobic Biodegradation of Plastic Materials in the Marine Environment by a Defined Microbial Consortium or Natural Sea Water Inoculum, 2018.
- 49 G. X. Wang, D. Huang, J. H. Ji, C. Völker and F. R. Wurm, *Adv. Sci.*, 2021, **8**, 2001121.
- 50 N. B. Erdal and M. Hakkarainen, *Biomacromolecules*, 2022, **23**, 2713–2729.
- 51 E. Castro-Aguirre, R. Auras, S. Selke, M. Rubino and T. Marsh, *Polym. Degrad. Stab.*, 2017, **137**, 251–271.
- 52 N. B. Halima, *RSC Adv.*, 2016, **6**, 39823–39832.
- 53 F. Kawai and X. Hu, *Appl. Microbiol. Biotechnol.*, 2009, **84**, 227–237.
- 54 M. T. Zumstein, A. Schintlmeister, T. F. Nelson, R. Baumgartner, D. Woebken, M. Wagner, H.-P. E. Kohler, K. McNeill and M. Sander, *Sci. Adv.*, 2018, **4**, eaas9024.
- 55 W. Purahong, S. F. M. Wahdan, D. Heinz, K. Jariyavidyanont, C. Sungkapreecha, B. Tanunchai, C. Sansupa, D. Sadubsarn, R. Alaneed and A. Heintz-Buschart, *Environ. Sci. Technol.*, 2021, **55**, 12337–12351.
- 56 P. K. Panda, K. Sadeghi and J. Seo, *Food Packag. Shelf Life*, 2022, **33**, 100904.
- 57 H. C. Erythropel, J. B. Zimmerman, T. M. de Winter, L. Petitjean, F. Melnikov, C. H. Lam, A. W. Lounsbury, K. E. Mellor, N. Z. Janković and Q. Tu, *Green Chem.*, 2018, **20**, 1929–1961.
- 58 T. Narancic, S. Verstichel, S. R. Chaganti, L. Morales-Gamez, S. T. Kenny, B. De Wilde, R. B. Padamati and K. E. O'Connor, *Environ. Sci. Technol.*, 2018, **52**, 10441–10452.
- 59 M. G. Mazzotta, C. M. Reddy and C. P. Ward, *Environ. Sci. Technol. Lett.*, 2021, **9**, 37–41.
- 60 A. Chamas, H. Moon, J. Zheng, Y. Qiu, T. Tabassum, J. H. Jang, M. Abu-Omar, S. L. Scott and S. Suh, *ACS Sustain. Chem. Eng.*, 2020, **8**, 3494–3511.
- 61 K. Park, S. Choe, K. Sadeghi, P. K. Panda, J. Myung, D. Kim and J. Seo, *Food Chem.*, 2024, **445**, 138772.
- 62 R. A. Sheldon, *Green Chem.*, 2023, **25**, 1704–1728.
- 63 R. A. Sheldon, *ACS Sustainable Chem. Eng.*, 2018, **6**, 32–48.
- 64 R. A. Sheldon, M. L. Bode and S. G. Akakios, *Curr. Opin. Green Sustainable Chem.*, 2022, **33**, 100569.
- 65 R. A. Sheldon, *Green Chem.*, 2014, **16**, 950–963.
- 66 M. Tosin, M. Weber, M. Siotto, C. Lott and F. Degli-Innocenti, *Front. Microbiol.*, 2012, **3**, 225.
- 67 R. J. Wright, G. Erni-Cassola, V. Zadjelovic, M. Latva and J. A. Christie-Oleza, *Environ. Sci. Technol.*, 2020, **54**, 11657–11672.
- 68 S. Chinaglia, M. Tosin and F. Degli-Innocenti, *Polym. Degrad. Stab.*, 2018, **147**, 237–244.
- 69 O. García-Depraect, R. Lebrero, S. Rodríguez-Vega, S. Bordel, F. Santos-Beneit, L. J. Martínez-Mendoza, R. A. Börner, T. Börner and R. Muñoz, *Bioresour. Technol.*, 2022, **344**, 126265.
- 70 E. Di Mauro, D. Rho and C. Santato, *Nat. Commun.*, 2021, **12**, 1–10.

